

Highlights

Reducing RES Droughts through the integration of wind and solar PV

Boris Morin, Aina Maimó Far, Damian Flynn, Conor Sweeney

- RES droughts are analysed using 45 years of hourly wind and solar PV generation data
- RES droughts from C3S-Energy and ERA5-Atlite datasets are compared
- Adding solar PV to a wind-dominated system reduces RES drought frequency and duration
- Validated RES datasets are crucial to accurately identify RES drought extremes

Reducing RES Droughts through the integration of wind and solar PV

Boris Morin^{a,*}, Aina Maimó Far^a, Damian Flynn^b, Conor Sweeney^a

*^aSchool of Mathematics and Statistics, University College Dublin, Belfield, Dublin
4, Dublin, D04 V1W8, Ireland*

*^bSchool of Electrical and Electronic Engineering, University College Dublin, Belfield,
Dublin 4, Dublin, D04 V1W8, Ireland*

*Corresponding author

Email addresses: `boris.morin@ucdconnect.ie` (Boris Morin),
`aina.maimofar@ucd.ie` (Aina Maimó Far), `damian.flynn@ucd.ie` (Damian Flynn),
`conor.sweeney@ucd.ie` (Conor Sweeney)

Abstract

Increasing the share of electricity produced from renewable energy sources (RES), combined with RES dependence on weather, poses a critical challenge for energy systems. This study investigates the importance of the balance between wind and solar photovoltaic (PV) capacity on periods of low renewable generation, known as RES droughts. Three different RES datasets are used to estimate the capacity factors for different scenarios of installed capacities for wind and solar PV power. The skill of the RES models is quantified by comparing capacity factor time series to observed hourly data and by assessing their representation of observed RES droughts. The RES models are used to generate a 45-year hourly time series of RES capacity factor, enabling analysis of the frequency, duration and return periods of RES droughts at a climatological scale. Results show the importance of using an accurate, validated RES model for RES drought risk assessment. The addition of solar PV capacity to a wind-dominated system results in a significant reduction in the frequency and duration of RES droughts, while also reducing extremes and seasonal RES drought patterns. These findings underscore the importance of diversification in RES capacity to enhance energy security and resilience.

Keywords: RES Drought, Wind Power, Solar PV Power, Renewable Energy Sources, Return Periods

1. Introduction

The EU aims to generate at least 69% of its electricity from renewable energy sources (RES) by 2030, up from 41% in 2022 [1]. While this transition is essential for reducing greenhouse gas emissions, it also highlights the challenge of managing the variability of weather-dependent energy sources such as wind and solar photovoltaic (PV) power. This challenge is amplified by the increasing electrification of energy sectors, which places greater demand on the power system and makes it more sensitive to meteorological conditions, both in historical [2] and future climates [3]. Periods of low renewable generation, known as *Dunkelflaute* or RES droughts, pose significant risks to system adequacy and energy security, emphasising the need for a resilient energy system to meet both growing electricity demand and decarbonisation targets.

RES drought events do not have a fixed definition, with various approaches present in the literature. One common method defines a RES drought as a period during which the average capacity factor (CF) remains below a fixed threshold for a specified duration. For example, Kaspar et al. [4] used this method to investigate the shortfall risks of low wind and solar PV generation in Europe, with a focus on Germany, testing multiple CF thresholds and durations. Similarly, Mockert et al. [5] examined the link between weather regimes and RES droughts in Germany using a 48-hour rolling window under a threshold to define RES droughts. Similar fixed-threshold approaches have also been applied using CF series reconstructed through machine learning in regions such as Japan [6] and Hungary [7].

Alternative methods adjust the CF threshold dynamically over the year to account for seasonal variations in renewable production. Raynaud et al. [8] defined RES droughts as sequences of days with renewable electricity generation below a threshold that varies seasonally, a methodology later adapted for India [9]. Building on this, Kapica et al. [10] compared the likelihood of increased RES droughts in Europe under different climate models. Other studies have defined RES droughts based on deviations from daily mean production: Rinaldi et al. [11] applied these in the U.S. Western Interconnection to quantify the benefits of long-term storage, while Brown et al. [12] examined weekly timescales to explore meteorological influences on the most severe RES drought events. Another method defines RES drought indices based on metrics commonly used in hydro-meteorology to characterise RES droughts [13]. ~~This index was also applied to the U.S. by Bracken et al. [14], revealing a consistent increase in the RES drought magnitude when load is considered, despite showing differing results across regions. The consideration of demand introduces a completely different factor to generation: weather is not the only driver, as the societal component plays a large role.~~ used this approach to analyse RES droughts at different time scales in the U.S. [14], and Lei et al. [15] used it to quantify RES droughts in wind-PV-hydro systems in China.

In addition to examining periods of low renewable electricity generation, several studies also explore the periods when the imbalance between renewable generation and electricity demand (residual ~~load~~ demand) is high. Raynaud et al. [8] ~~defined both energy production and energy supply droughts, and showed the difference in their patterns~~ between RES droughts and high

52 residual demand events in a hypothetical fully renewable system composed
 53 of wind, solar PV and run-of-the-river hydropower. Similarly, Allen and
 54 Otero [13] also defined a standardised index based on meteorological droughts
 55 to address residual ~~load~~demand, whose correlation to the ~~energy production~~
 56 electricity generation index is mostly negative (as expected, although quite
 57 low anticorrelations and even small positive correlations appear for some Eu-
 58 ropean countries). This index was also applied to the U.S. by Bracken et
 59 al. [14], revealing a consistent increase in the RES drought magnitude when
 60 ~~load~~demand is considered, despite showing differing results across regions.

61 In this paper, the focus is exclusively on renewable electricity genera-
 62 tion, ~~which allows us to maintain physical models that do not consider~~
 63 ~~the behavioural influence of demand, whose role will be addressed in the~~
 64 ~~discussion~~to keep the focus on RES droughts driven by the weather. A fixed
 65 threshold approach is used to define RES droughts, which facilitates con-
 66 sistent inter-comparison between scenarios with different installed wind and
 67 solar PV capacities. The case study used in this paper is Ireland, a region
 68 ~~with a strong reliance on~~where most RES generation comes from wind power
 69 and with ambitious targets for solar PV power expansion. This provides valu-
 70 able insights into the potential benefits of ~~diversifying the renewable energy~~
 71 ~~mix on RES droughts in the context of realistic scenarios~~adding solar PV
 72 installations in wind-dominated countries.

73 RES droughts are identified using onshore wind and solar PV CF time
 74 series. In this study, three different datasets are used and compared, all of
 75 which are driven by the ERA5 reanalysis [16]. Two of the datasets are part
 76 of C3S Energy (C3SE), an energy-based operational dataset produced by
 77 the EU Copernicus Climate Change Service [17]. One of the C3SE datasets
 78 provides CF time series aggregated at the national scale, while the other
 79 provides the CF time series at each grid point, at the ERA5 resolution of
 80 0.25°. The third dataset produced by the authors was generated using the
 81 Atlite model [18], which converts the ERA5 atmospheric data to a generation
 82 time series using specified wind turbine and PV panel models. Atlite is an
 83 open-source tool developed by PyPSA [18] and has been used for estimating
 84 wind and solar PV generation in order to study RES droughts in Germany [5].

85 Generic datasets for wind and solar PV CF are often used for the quan-
 86 tification of RES droughts. Despite undergoing a validation process, they
 87 are often not fully representative of each geographical location, and can
 88 show differences in the number of RES drought events[19]. ~~In this work,~~
 89 ~~we quantify~~ [19]. This study evaluates the skill of a dataset developed for

90 the European region (C3SE) ~~when used for~~ when applied to a specific coun-
91 try ~~(Ireland)~~. In particular, ~~we investigate~~ the analysis explores the impact of
92 using a generic versus a tailored dataset on ~~the analysis of RES droughts~~ RES
93 drought assessments, in the context of a transition from a wind-dominated
94 system to one with a ~~larger~~ greater share of solar PV capacity.

95 The aim of this study is to answer ~~three~~ two questions which are relevant
96 for systems with a large share of RES generation:

- 97 • Do generic datasets have sufficient skill to reliably quantify ~~extreme~~
98 RES drought events?
- 99 • ~~What is the importance of using accurate RES farm locations, and~~
100 ~~regionally-validated wind and solar PV models, when analysing of RES~~
101 ~~droughts?~~
- 102 • How does the integration of solar PV capacity into a predominantly
103 wind-based system alter the characteristics of RES drought events?

104 The datasets used in this study are detailed in section 2, which describes
105 their characteristics and relevance for evaluating RES droughts. Section 3
106 outlines the RES datasets used to simulate wind and solar PV generation and
107 provides the methodology for defining and identifying RES drought events,
108 including the thresholds and metrics applied. In section 4, the datasets are
109 first verified against observed energy data to assess their accuracy, followed by
110 an analysis of RES drought occurrences for two scenarios with different ratios
111 of installed wind to solar PV capacities. Finally, section 5 offers a discussion
112 of the results in the context of energy reliability and future planning, followed
113 by the main conclusions and recommendations for further research.

114 2. Data

115 This study uses publicly available datasets to construct and validate the
116 datasets for estimating the CF of wind and solar PV power. The primary
117 data sources include: EirGrid and SONI, the transmission system operators
118 (TSO) for the Republic of Ireland and Northern Ireland, respectively; the
119 ERA5 reanalysis dataset; and the C3SE dataset.

120 2.1. Wind and solar PV Capacity and Availability

121 EirGrid, the TSO for the Republic of Ireland, and SONI, the Northern
 122 Ireland TSO, provide detailed datasets on all wind and solar PV farms across
 123 the island of Ireland (Republic of Ireland and Northern Ireland) from 1990
 124 to the present [20]. These datasets include information such as each farm’s
 125 installed capacity, name, and connection date. To enhance the accuracy of
 126 this data, the longitude and latitude for each farm were manually determined
 127 through online searches. For simplicity, this data will be referred to as orig-
 128 inating from EirGrid, as all-island data was directly obtained from EirGrid,
 129 and the combined regions of the Republic of Ireland and Northern Ireland
 130 will be referred to as Ireland throughout the remainder of this document.

131 The spreadsheet available from the EirGrid website contains two key vari-
 132 ables: generation and availability. Generation is the energy that a RES farm
 133 actually contributed to the grid, which may include limitations introduced
 134 by the TSO to maintain grid stability, such as constraints and curtailment.
 135 Availability represents the energy that would have been generated from a RES
 136 farm if no grid constraints had been applied, making it representative of the
 137 weather-related response. Generation and availability values are available
 138 from 2014 onward for wind power and from 2018 onward for solar PV power,
 139 although solar PV availability data only became present in the Republic of
 140 Ireland in 2023. This study focuses on availability for all analyses.

141 2.2. Atmospheric Variables

142 All of the datasets used in this study are driven by data from the ERA5 re-
 143 analysis [16], produced by the European Centre for Medium-Range Weather
 144 Forecasts (ECMWF). This global gridded dataset provides hourly atmo-
 145 spheric variables from 1940 to the present at a horizontal resolution of 0.25°.
 146 Table 1 lists the relevant ERA5 variables.

Table 1: ERA5 variables used to calculate wind and solar PV generation

ERA5 name	variable
100 metre zonal and meridional wind speed	u_{100}, v_{100}
2 metre temperature	$t2m$
Surface net solar radiation	ssr
Surface solar radiation downwards	$ssrd$
Top of atmosphere incident radiation	$tisr$
Total sky direct solar radiation at surface	$fdir$

147 2.3. C3S Energy

148 The EU Copernicus Climate Change Service developed the C3S-Energy
149 (C3SE) renewable energy dataset for Europe [17], using ERA5 atmospheric
150 variables and weather-to-energy models. This dataset provides hourly CF
151 for wind and solar PV ~~energy~~ power from 1979 to the present. The data
152 are available on the same grid as the ERA5 data, which has a horizontal
153 resolution of 0.25° . The time series are also available for download at two
154 aggregated scales: regional (NUTS 2) and national.

155 The wind CF in C3SE was calculated using wind speeds at 100 metres
156 (u_{100}, v_{100}) and a standard turbine model, the Vestas V136/3450, with a fixed
157 hub height of 100 metres. As data on wind turbine fleet locations and speci-
158 fications are difficult to obtain across Europe, C3SE assumes a homogeneous
159 distribution of wind turbines across the ERA5 grid. While this approach
160 does not capture the precise capacity factors reported by grid operators, it
161 provides a well-correlated time series that effectively represents the impact
162 of climate variability on wind power generation. The C3SE solar PV CF was
163 also calculated for the ERA5 grid. It is derived from meteorological data, in-
164 cluding surface solar radiation downwards ($ssrd$) and air temperature ($t2m$),
165 using a reference solar PV plant model. This model incorporates empirical
166 calculations for key system components such as optical losses, module effi-
167 ciency, and inverters. The final CF accounts for a mix of module orientations
168 typical for each location [21].

169 3. Methods

170 This study ~~uses~~ analyses RES droughts using onshore wind and solar
171 PV CF time series from three datasets ~~to analyse RES droughts across the~~
172 ~~island of Ireland. Data downloaded:~~ two from C3SE ~~were used to obtain~~
173 ~~two datasets: one~~, based on national-level data (C3S NAT) ~~, and another~~
174 ~~on and~~ grid-level data (C3S GRD). ~~The third dataset was computed using,~~
175 and one derived from the Atlite model (ATL).

176 3.1. C3S Energy National: C3S NAT

177 The C3S NAT dataset is created by combining two inputs provided by
178 C3SE at the corresponding NUTS levels: Republic of Ireland (NUTS0: IE)
179 and Northern Ireland (NUTS2: UKN0). The two inputs are combined, using
180 the actual installed capacity as weights. This dataset assumes that RES
181 generation occurs at every ERA5 grid point in Ireland.

182 3.2. C3S Energy Gridded: C3S GRD

183 The C3S GRD dataset uses, as inputs, the actual locations of the RES
184 farms in Ireland, and the CF from C3SE over the ERA5 grid. For each
185 farm, the CF from the nearest grid point on the C3SE dataset was selected.
186 A weighted average of the CF associated with each farm, using the farm's
187 installed capacities, was used to produce the total CF time series.

188 3.3. Atlite: ATL

189 The ATL dataset is produced using the Atlite model. Atlite allows the
190 user to define the wind turbine power curve and PV panel model to use
191 when converting weather variables to wind and solar PV generation. The
192 Atlite model takes as inputs the locations of RES farms and ERA5 weather
193 variables: wind speed at 100 metres (u_{100} , v_{100}) for wind generation, and
194 radiation variables (ssr , $ssrd$, $tisr$, and $fdir$) along with air temperature
195 ($t2m$) for solar PV generation. The output of the Atlite model is a generation
196 time series, which is divided by the total capacity to transform it back into
197 CF. The selection of the wind turbine power curve and PV panel model
198 represents the key difference between this dataset and C3S GRD. This study
199 identifies the most appropriate wind turbine power curve to use from the
200 121 power curves, each at five different levels of smoothing, made available
201 by Renewables.ninja [22], and selects the PV panel model out of the options
202 available within Atlite.

203 3.4. Energy Scenarios

204 The three datasets provide CF time series for both wind and solar PV. In
205 addition to analysing the CF of wind and solar PV separately, a combined
206 CF was computed for each dataset by averaging wind and solar PV CF,
207 weighted by their installed capacities at the end of 2023 (5.9 GW for wind
208 power and 0.6 GW for solar PV power). This configuration is referred to as
209 the 91W-9PV scenario, reflecting the distribution of 91% wind and 9% solar
210 PV capacity. Given that solar PV capacity in Ireland is low in 2023, and to
211 explore how a more balanced distribution of wind and solar PV capacities
212 might impact RES droughts, this study also considered a second scenario,
213 referred to as 57W-43PV, where the installed solar PV capacity is assumed
214 to increase to 8.6 GW, while wind capacity rises to 11.45 GW. These values
215 are based on targets outlined in the roadmap published by the 2024 Climate
216 Action Plan [23]. This study does not include offshore wind in the analysis.
217 Recent reports suggest that even by 2030, Ireland is unlikely to have any

218 significant new offshore wind farms, with projected offshore capacity expected
219 to remain near zero using realistic scenarios [24].

220 New time series were generated for both the ATL and C3S GRD solar
221 PV datasets, incorporating a revised distribution of installed capacity across
222 Ireland as specified in the roadmap. For wind power, the CF time series
223 remains unchanged, as significant shifts in the location of wind farms are not
224 expected. In total, twelve CF time series were analysed in this study, six for
225 individual wind and solar PV CF (three datasets for each source) in the 91W-
226 9PV scenario, and an additional six time series that include the combined
227 CF for 91W-9PV and 57W-43PV scenarios across the different datasets.

228 It is important to note that the specific capacity values used in this study
229 are illustrative and are not intended to reflect ~~precise~~-accurate future reali-
230 ties. Instead, they serve to explore the impact of transitioning from a wind-
231 dominated system (91W-9PV) to a more evenly distributed system (57W-
232 43PV). This approach allows for a comparative analysis between the two
233 scenarios, assessing how the balance of RES capacity affects the occurrence
234 of RES droughts.

235 For each dataset (ATL, C3S GRD, and C3S NAT), four distinct scenarios
236 are examined, as summarised below:

- 237 • Wind Power - based on the actual capacity at the end of 2023
- 238 • Solar PV Power - based on the actual capacity at the end of 2023
- 239 • Combined RES / 91W-9PV - based on the actual capacity at the end
240 of 2023
- 241 • Combined RES / 57W-43PV - based on the projected capacity for 2030

242 3.5. RES Drought Definition

243 In this study, a RES drought event was defined as occurring when the
244 24-hour moving average of CF remains below a fixed threshold of 0.1 for a
245 period of longer than 24 hours. By using a 24-hour moving average, fewer
246 but longer-lasting events were captured compared to using the raw CF time
247 series, which can be more sensitive to short-term fluctuations. The 24-hour
248 rolling average also avoids potential masking of day-long events due to their
249 start time. A fixed threshold approach was chosen in this study to enable
250 consistent inter-comparison between datasets.

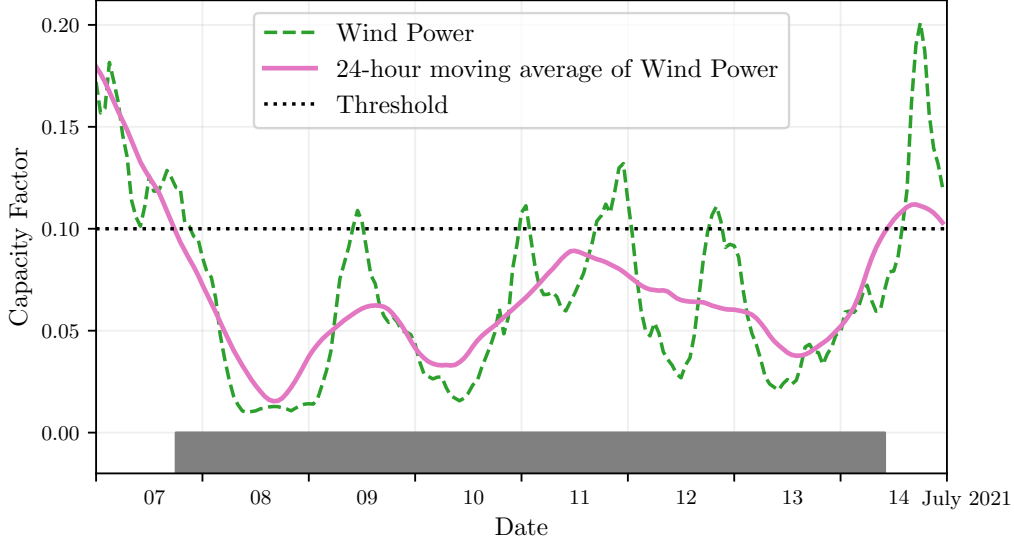


Figure 1: Wind time series of CF (green) and its 24-hour moving average (pink) from the 7th to the 15th of July 2021. The black dashed line indicates the CF threshold. The grey bar shows the period identified as a wind drought under our definition

251 The moving average approach smooths out short-term fluctuations, so
 252 that brief periods above the threshold do not interrupt an otherwise continu-
 253 ous low-CF period (Fig. 1). This means that a single hour above the threshold
 254 does not "break" a RES drought event if it is surrounded by prolonged low-
 255 generation hours. As a result, fewer but longer-lasting RES drought events
 256 are identified, which may better reflect ~~real-world~~ actual conditions where
 257 energy supply constraints persist over extended periods.

258 4. Results

259 4.1. Verification

260 The accuracy of the datasets used in this study was verified, before con-
 261 tinuing to the analysis of RES droughts. For the verification process, time-
 262 varying values of installed capacity were used to account for changes in RES
 263 development over the verification period. This step allowed us to assess how
 264 well the datasets represent the production of renewable energy by compar-
 265 ing them against observed data. This validation step evaluates how well the
 266 datasets represent actual renewable energy production by comparing them

267 against observed data. The overall statistical distribution of CF values for
 268 wind (2014–2023) and solar PV (2023) is presented in the violin plots in
 269 Fig. 2. These plots illustrate the density of CF values for each dataset,
 270 highlighting their differences and alignment with observations. The results
 271 indicate that ATL aligns more closely with OBS for wind, while all datasets
 272 exhibit similar distributions for solar PV.

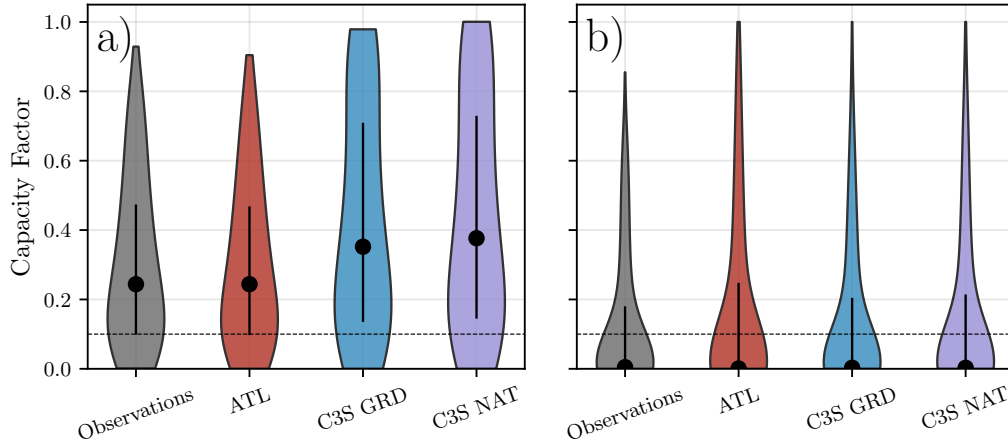


Figure 2: Violin plots of CF distributions for wind a) and solar PV b) for the Observations (grey) and the three datasets: ATL (red), C3S GRD (blue), and C3S NAT (purple). The black dot shows the median values, while the black vertical lines represent the first and third quartiles. The red line indicates the threshold of 0.1 used in the study to identify RES droughts

273 4.1.1. Wind Energy

274 The C3S datasets use the Vestas V136/3450 wind turbine power curve
 275 (Fig. 3a). The Atlite model allows the user to specify the power curve.
 276 We considered the 121 power curves available for download from Renew-
 277 ables.ninja [22]. For each power curve, Renewables.ninja also provides four
 278 associated smoothed power curves. The smoothing is done using a Gaussian
 279 filter with different standard deviations that depend on the wind speed. A
 280 separate wind CF time series for Ireland was generated for each of the wind
 281 turbine power curves and smoothing levels.

282 The performance of each CF time series is then assessed based on four skill
 283 scores: correlation coefficient (CC), root mean square error (RMSE), mean
 284 bias error (MBE), and the percentage of overlap. The percentage of overlap

285 quantifies the similarity between the observed and modelled distributions. It
 286 is a positively oriented skill score, where 100% shows full agreement between
 287 the two distributions, and 0% indicates no overlap. The histograms of hourly
 288 CF values for the most recent decade (2014-2023) are used to calculate this
 289 skill score.

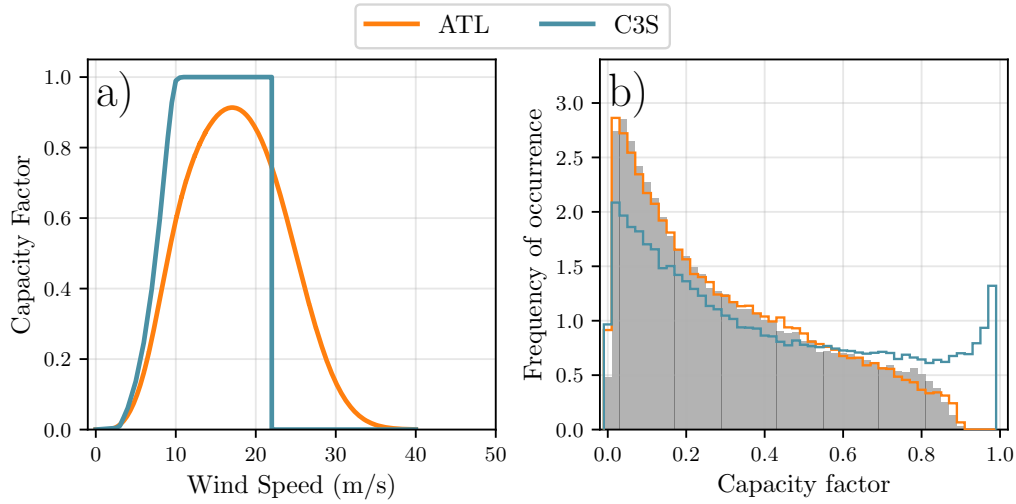


Figure 3: a) Power curves of the Enercon E112.4500 with a $0.3w$ smoothing filter used by the ATL dataset (orange) and the Vestas V136/3450 used by C3SE-the two C3S datasets (blue) b) Histograms of wind CF for Ireland from the ATL dataset (orange), C3SE-the C3S datasets (blue) and Observed (shaded)

290 Based on these metrics, the most representative power curve for Ireland
 291 is the Enercon E112.4500 power curve with the $0.3w$ smoothing filter. The
 292 smoothing of the wind turbine power curve represents losses associated with
 293 each turbine, as well as losses such as wake effects between turbines, which
 294 are important when modelling wind energy on larger spatial scales. The
 295 histogram in Fig. 3b shows that the C3SE power curve tends to underestimate
 296 low CF values and overestimate higher ones, whereas the smoothed ATL
 297 power curve more closely follows the observed wind availability data. This
 298 is further supported by the percentage of overlap which is higher for ATL
 299 (97.2%) than for C3SE (83.2%), indicating better agreement with observed
 300 data.

301 The effect of the difference between the power curves is also visible in
 302 Fig. 4, which shows a density plot of wind CF values. The two C3S datasets

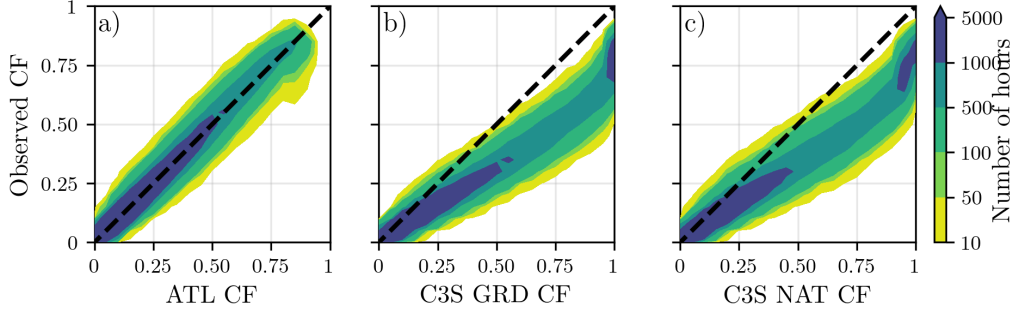


Figure 4: Wind CF density plot of the observed CF (vertical axes) and modelled (horizontal axes) CF data for the a) ATL, b) C3S GRD and c) C3S NAT datasets

are shown to overestimate the observed CF, whereas the ATL dataset is in good agreement with the observed data. The skill scores presented in Table 2 show that ATL performs better than the two C3S datasets for all of the skill scores.

	ATL	C3S GRD	C3S NAT
CC	0.981	0.972	0.970
RMSE	0.045	0.177	0.162
MBE	-0.003	0.137	0.121

Table 2: Skill scores for wind power for the three datasets compared to observed data

Fig. 5 shows the average annual number of wind drought events during the 2014 to 2023 validation period. The figure reveals that ATL presents the best overall agreement with the observed frequency and duration of wind drought events. This pattern is particularly evident for shorter-duration events, which are the most frequent.

This verification for wind generation data highlights the importance of selecting a representative wind turbine power curve for the region being analysed. The ATL dataset, which uses a representative wind turbine power curve, is skilled at reproducing wind CF and RES droughts over Ireland. On the other hand, the power curve used for both C3S GRD and C3S NAT is not representative for Ireland, as it severely overestimates generation, underestimating the occurrence of RES droughts. This highlights a problem with using generalised datasets for analysing RES droughts: biases severely affect their ability to accurately reproduce RES drought events. The skill

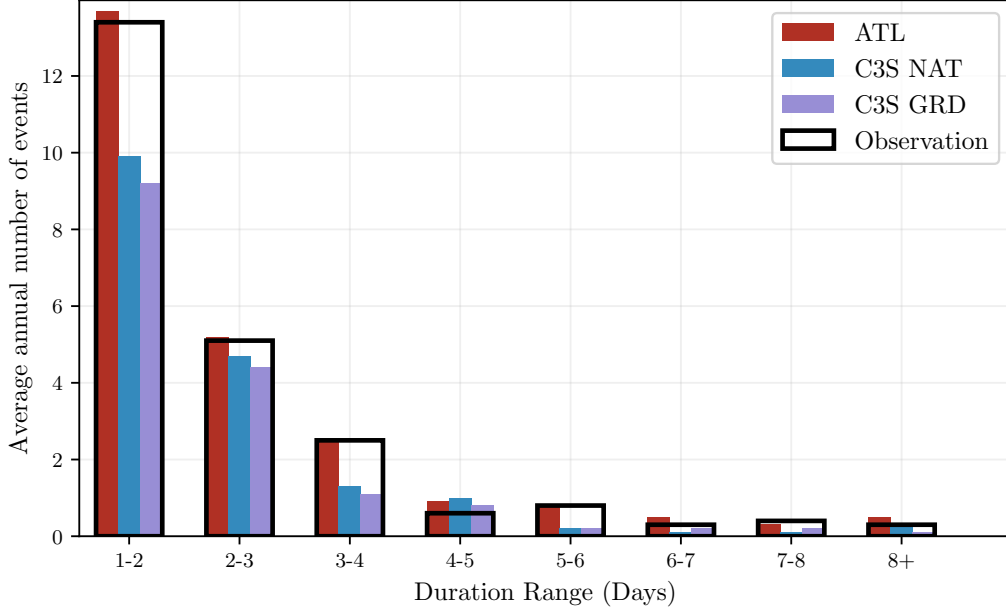


Figure 5: Average annual number of wind drought events for ATL (red), C3S GRD (blue), C3S NAT (purple), and the observed data (black outline). The wind droughts are identified from 2014 to 2023, considering the actual capacity of the system at any given time

321 scores for the three datasets (Tab. 2) show only a small difference in their
 322 ability to reproduce the changes in CF, as seen by their similar CC scores.
 323 However, their ability to reproduce the actual CF values is much lower than
 324 that of ATL, with RMSE scores almost four times bigger for the two C3S
 325 datasets. There is a clear bias towards an overestimation of CF, seen in
 326 the MBE values, which leads to the underestimation of RES droughts. This
 327 highlights the need to use regionally verified models to assess RES droughts.

328 4.1.2. Solar PV Energy

329 The Atlite model allows the user to select certain PV panel characteristics.
 330 In this study, the three PV panel types available in the Atlite model were
 331 considered (CSi, CdTe, Kaneka). Following the same methodology as in the
 332 previous section, the three available models were compared using four skill
 333 scores (CC, RMSE, MBE, and the percentage of overlap). Based on the best-
 334 performing metrics, the Beyer PV panel model was selected [25], using the
 335 Kaneka Hybrid panel option. For all solar PV farm locations, the azimuth
 336 angle is fixed at 180°(due south), and the optimal tilt angle option is applied.

337 The solar PV installed capacity available on the spreadsheets from Eir-
 338 Grid represents the Maximum Export Capacity (MEC) and does not ac-
 339 curately reflect the installed solar PV capacity. To enable actual solar PV
 340 generation potential to be modelled correctly, installed capacities were set at
 341 1.4 times the MEC values. This scaling factor was estimated by analysing
 342 proprietary data from individual solar PV farms provided by EirGrid, which
 343 showed that, on average, assuming that the installed capacities of farms ex-
 344 ceed their MEC values by 40% yields the best agreement with the observed
 345 availability.

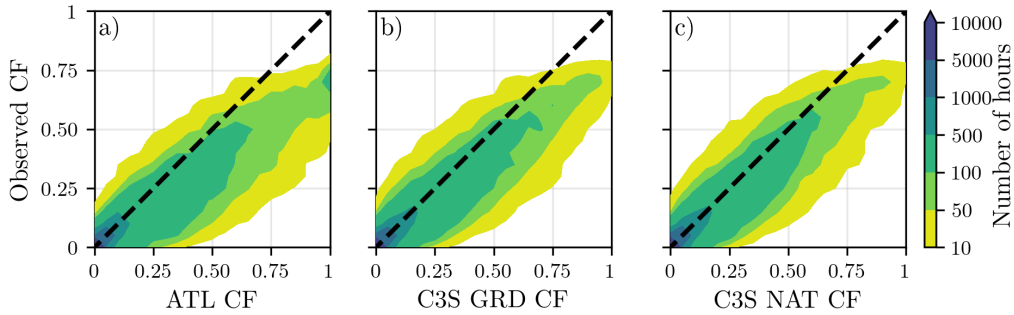


Figure 6: Solar PV CF density plot of the observed (vertical axes) and modelled (horizontal axes) CF series for the a) ATL, b) C3S_{GRD} and c) C3S_{NAT} datasets

346 Fig. 6 shows that the three datasets have a similar tendency to overesti-
 347 mate the CF compared to the observed values, especially for high CF values.
 348 The skill scores presented in Table 3 indicate that C3S_{GRD} and C3S_{NAT}
 349 perform better than ATL for solar PV CF, with lower RMSE and MBE,
 350 and higher CC scores. This may be due to the statistical approach taken by
 351 C3SE for the orientation of the PV panels.

	ATL	C3S _{GRD}	C3S _{NAT}
CC	0.921	0.931	0.931
RMSE	0.119	0.090	0.113
MBE	0.046	0.027	0.021

Table 3: Skill scores for solar PV CF for the three datasets compared to observed data

352 Fig. 7 shows the number of solar PV drought events during the 2023
 353 validation period across different duration ranges. The figure reveals partial

354 agreement between the three datasets and the observed data, with consistent
 355 results noticed for duration ranges of 1-2, 3-4, 7-8, and 8+ days. However,
 356 discrepancies appear in the other ranges, where the models diverge from the
 357 observed data. The main challenge in validating solar PV data stems from
 358 the recent installation of a large share of Ireland's solar PV capacity, with
 359 over 65% of the total solar PV capacity installed in 2023. This results in
 360 uncertainties in solar PV generation data and the actual generating capacity
 361 in the first few months after each farm is connected. Overall, C3S GRD
 362 performs slightly better than the other datasets in reproducing observed solar
 363 PV drought events.

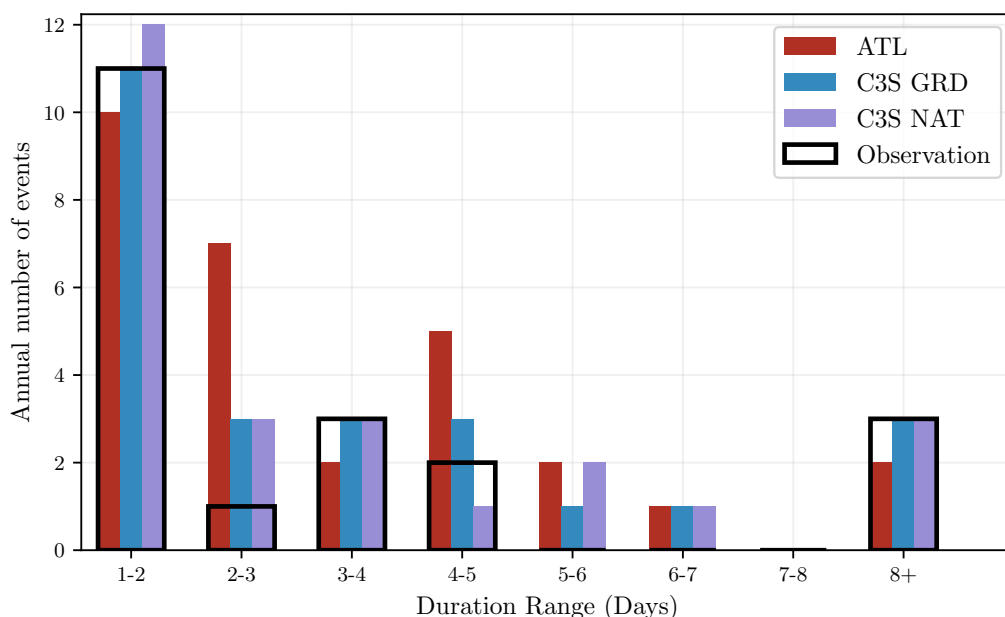


Figure 7: Number of solar PV drought events for ATL (red), C3S GRD (blue), and C3S NAT (purple) and the observed data (black outline). The solar PV droughts are identified for 2023, considering the actual capacity of the system at any given time

364 4.2. Analysis

365 In this section, RES droughts are analysed by calculating the frequency
 366 and duration of RES drought events, the return periods for different RES
 367 drought durations, and the seasonality of RES drought events. Understand-
 368 ing the characteristics and timing of RES drought events enables system op-

erators to optimally plan for reserve capacity requirements, ensuring grid stability and security of supply. Results are presented for the three datasets, allowing their differences on the characterisation of RES droughts to be clearly identified.

RES drought events are evaluated under two different scenarios with fixed installed capacities: the 91W-9PV scenario, with 5.9 GW of wind capacity and 0.6 GW of solar PV capacity; and the 57W-43PV scenario, where wind capacity comprises 11.45 GW and solar PV capacity increases to 8.6 GW. Both scenarios were driven by 45 years of ERA5 data. Using the RES drought identification process described in Section 3.5, wind and solar PV droughts are first analysed separately before presenting the results for combined (wind + solar PV) RES droughts under both scenarios.

4.2.1. Annual Number of RES Droughts

The first part of the analysis examines the annual number of RES drought events. When only wind energy is considered (Fig. 8a), the number of RES drought events decreases as the duration range increases, with very few events lasting more than seven days. In contrast, for solar PV energy (Fig. 8b), RES drought frequency declines from one to eight days and then slightly increases for longer durations. This behaviour is attributable to Ireland’s high-latitude location, where reduced sunlight in winter (from November to March) leads to consistently low solar PV output.

Moreover, the comparison between wind and solar PV results indicates that the median, first, and third quartiles for solar PV are consistently higher than or equal to those for wind. This is expected, given that solar PV generation is inherently lower, zero at night, and limited by the solar cycle. When wind and solar PV are combined under the 91W-9PV scenario (Fig. 8c), the results closely mirror those of wind alone, due to the dominance of wind power in the current energy mix. However, in the 57W-43PV scenario (Fig. 8d), a marked reduction in RES drought events is observed across all datasets, with a decrease of the total number of events of 56% for ATL, 52% for C3S GRD, and 50% for C3S NAT, demonstrating the beneficial effects of a more balanced energy mix.

The consistently higher RES drought counts reported by the ATL dataset, compared to the C3S datasets, underscore the importance of wind turbine power curve representation when quantifying RES droughts. Whereas the three datasets agree on the overall effect of balancing the share of wind and solar PV generation, they differ at a quantitative level, which has crucial

406 implications for energy planning.

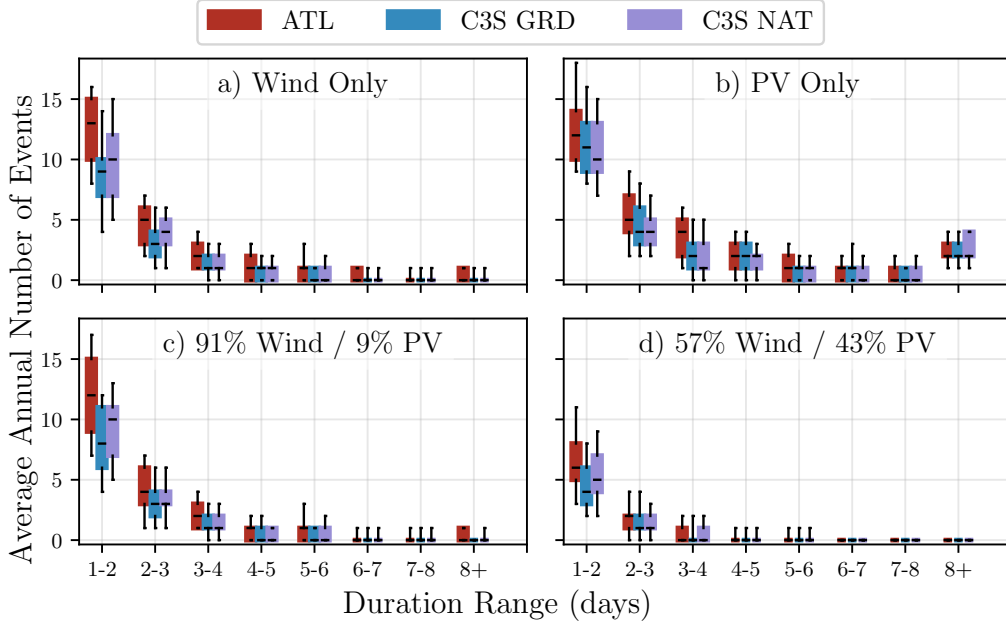


Figure 8: Average annual number of RES droughts (from 1979 to 2023) for a) Wind, b) solar PV, c) 91W-9PV and d) 57W-43PV for ATL (red), C3S GRD (blue), and C3S NAT (purple). The x-axis represents duration ranges in days (lower bound included), while the y-axis indicates the annual number of events. The boxes display the first and third quartiles and the median is marked by a black line. The whiskers indicate the 5th and 95th percentiles

407 4.2.2. Return Periods of RES Drought Duration

408 RES drought events identified over the 45-year period were used to cal-
 409 culate the return periods for different RES drought durations. A return
 410 period is the estimated average time interval between events of a specified
 411 duration (not to be confused with the frequency of their occurrence within a
 412 fixed time frame). Fig. 9 shows the return periods for different RES drought
 413 durations, which can be used to capture the most extreme events affecting
 414 the system. Understanding their return periods is crucial, as extreme yet
 415 rare RES droughts pose the toughest challenge to energy security by placing
 416 significant strain on the conventional backup sources necessary to maintain
 417 security of supply during these events.

418 The duration of wind droughts (Fig. 9a) increases in a log-linear fashion
 419 across the three datasets. The log-linear trend indicates a predictable rela-
 420 tionship between wind drought duration and occurrence, with longer wind
 421 droughts becoming exponentially less likely as duration increases. In the
 422 case of solar PV droughts (Fig. 9b), Atlite behaves differently than the two
 423 C3S datasets. The ATL dataset show a generally log-linear increase. For
 424 C3S GRD and C3S NAT, the duration of PV droughts increases in a log-
 425 linear pattern for events lasting less than 16 days. Beyond this duration,
 426 there is a sharp rise in solar PV drought duration for events up to a one-year
 427 return period. This sudden increase again reflects the impact of extended
 428 periods of low PV generation during winter in Ireland. The difference be-
 429 tween the ATL and the C3S results arises from differences in the datasets
 430 near the threshold of 0.1 CF. ATL remains slightly above the threshold more
 431 frequently during these conditions, leading to shorter, more fragmented RES
 432 drought events. In contrast, C3S GRD and C3S NAT tend to fall below the
 433 threshold in similar conditions, resulting in longer continuous RES drought
 434 periods, especially during winter.

435 Under the 91W-9PV scenario (Fig. 9c), the combined RES drought return
 436 periods mirror those for wind alone, reflecting the dominance of wind in the
 437 current energy mix. In contrast, the 57W-43PV scenario (Fig. 9d) shows
 438 a dramatic increase in return periods across all durations, suggesting that
 439 a more diversified energy mix can substantially mitigate the frequency of
 440 prolonged RES drought events. For example, the return period for a five-day
 441 RES drought event (shown by the vertical dashed lines in Fig. 9) extends
 442 from roughly six months for the 91W-9PV scenario, to four years for the
 443 57W-43PV scenario in the ATL dataset, and from about fifteen months to
 444 around five years in the two C3S datasets. Despite the lower wind share in the
 445 57W-43PV scenario, typically known for its relative stability, the balanced
 446 share with solar PV leads to extended return periods for RES droughts. This
 447 result indicates that the complementarity between wind and solar PV plays a
 448 crucial role in reducing the occurrence of RES drought events in a diversified
 449 energy portfolio.

450 Across Fig. 9a, c, and, d, the return periods in the ATL dataset are con-
 451 sistently higher than those in the two C3S datasets. For instance, in the
 452 91W-9PV scenario (Fig. 9c), an event with a one-year return period lasts six
 453 days in the ATL dataset, compared to only five days in the C3S datasets.
 454 This difference underscores the importance of model selection when quan-
 455 tifying RES droughts, as each dataset’s assumptions and parametrisations

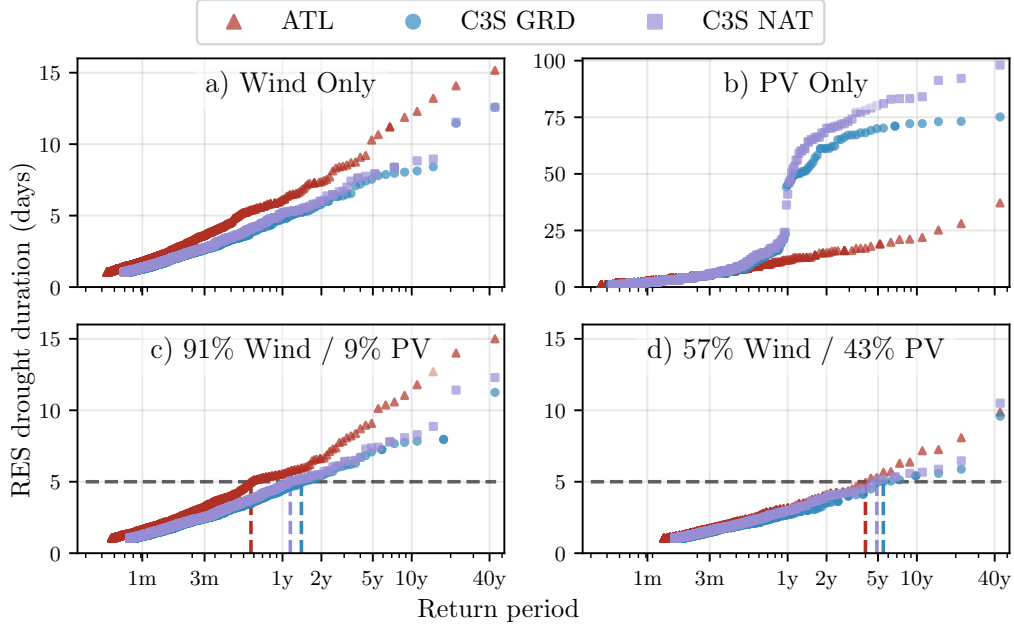


Figure 9: Return periods of the duration of RES droughts (from 1979 to 2023) for a) Wind, b) Solar PV, c) 91W-9PV and d) 57W-43PV for ATL (red triangle), C3S GRD (blue circle), and C3S NAT (purple square). The x-axis represents the return period time in a log-scale and the y-axis indicates the duration of RES drought associated with it. The horizontal dashed line marks the 5-day return period, with coloured vertical dashed marking its return period for each dataset

significantly influence RES droughts duration estimates. Additionally, in all four graphs, the similarity between results from the two C3S datasets suggests that assumptions in the ATL dataset, such as wind turbine power curve selection and PV panel specifications, have a greater impact on RES drought duration estimates than the precise geographic distribution of RES farms when studying the return periods of RES droughts.

The return periods calculated from the three datasets show large differences, in particular for the more extreme events with longer return periods. The C3S datasets produce shorter RES drought durations for these events, which would have the largest impact on the power system. This shows that system planning based on the wrong datasets could yield an underestimation of the duration of extreme RES droughts, potentially leading to shortages linked to undersized reserve capacity.

4.2.3. Seasonal Distribution of RES Droughts

The seasonal analysis of RES droughts is based on the percentage of hours in each month classified as part of a RES drought event. Wind droughts tend to be more frequent during summer, whereas solar PV droughts are more common in winter due to reduced sunlight. By comparing these seasonal patterns across different datasets and energy scenarios, this study examines how model-specific assumptions and variations in capacity mix affect the overall characterisation of RES drought events.

For the wind-only scenario (Fig. 10a), the ATL dataset exhibits a pronounced seasonal pattern, with about 24% of summer hours (June, July, August) identified as RES droughts compared to only 4% in winter (December, January, February). This strong seasonal signal is less evident in the C3S datasets, which suggests that the differences in the underlying wind power curves play a significant role. In ATL, CF near or below the 0.1 threshold occurs at relatively higher wind speeds, resulting in a higher count of RES drought hours during the summer months. In contrast, solar PV droughts (Fig. 10b) display an opposite seasonal trend. Across all datasets, over 60% of winter hours are classified as solar PV droughts, reflecting the naturally low solar irradiance in Ireland during winter.

ATL tends to record a slightly higher percentage of RES drought hours for wind and a marginally lower percentage for solar PV relative to the C3S datasets. These differences highlight how dataset-specific assumptions, such as the treatment of wind turbine power curves and PV panel characteristics, significantly influences the apparent seasonal dynamics of RES droughts.

The 91W-9PV scenario (Fig. 10c) shows patterns comparable to the ones for wind droughts (Fig. 10a). However, in the 91W/9PV scenario, the number of hours classified as RES droughts in summer decreases slightly compared to the wind-only scenario. This reduction can be explained by the contribution of solar PV generation during the summer months in the 91W-9PV scenario, even though it constitutes only 11% of total capacity. Since the number of RES drought hours for solar PV in summer is near zero, this small contribution has a noticeable impact on reducing overall RES drought hours. In the 57W-43PV scenario (Fig. 10d), all three datasets show a reduction in monthly RES drought frequency. Annual reductions in median RES drought frequency are observed across the datasets, dropping from 14% to 5% for ATL, from 8% to 3% for C3S GRD, and from 9% to 4% for C3S NAT. The balanced mix of wind and solar PV power in this scenario reduces the sea-

sonal signal overall and significantly decreases the percentage of RES drought hours in the summer.

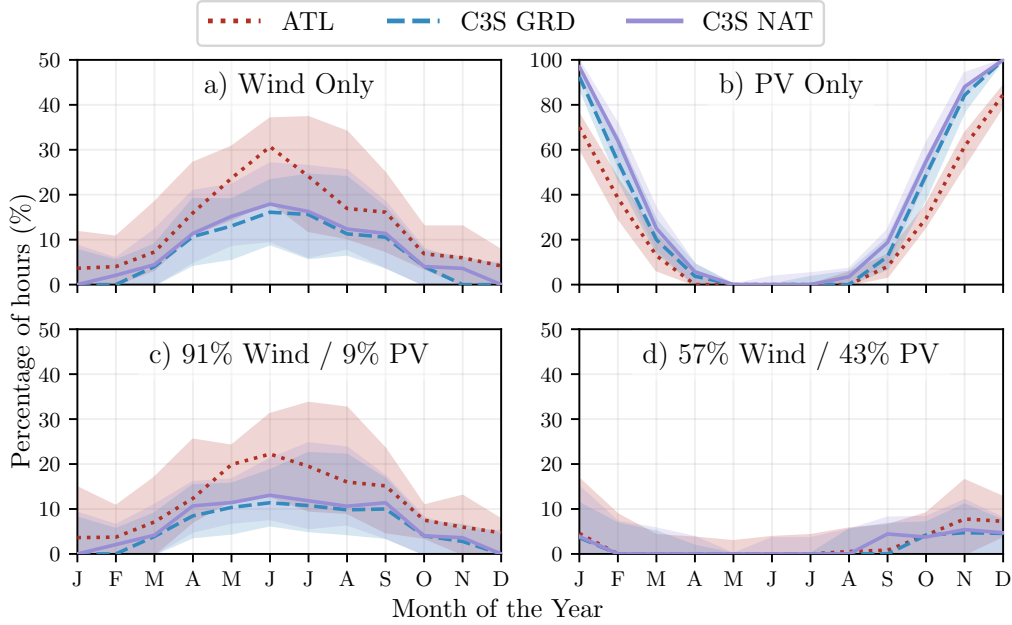


Figure 10: Percentage of hours in a month which are part of a RES drought (from 1979 to 2023) for a) Wind, b) Solar PV, c) 91W-9PV and d) 57W-43PV for ATL (red dotted), C3S GRD (blue dashed), and C3S NAT (purple solid). The x-axis represents the month of the year, and the y-axis indicates the percentage of hours. Lines correspond to the median values and the area between the first and third quartiles is shaded. Note the different y-axis scale for b).

The seasonal variations of RES droughts observed in this study have important implications for energy planning. Energy demand peaks in winter for Northern European countries, making the seasonality of RES droughts critical for the sizing of reserve capacity. Our results show that selecting the wrong dataset could severely underestimate RES droughts during winter months, thereby affecting the reliability of the energy system during critical periods. Additionally, the integration of large shares of solar PV in the system leads to a generalised reduction of RES droughts, yet winter months present a slight increase. The natural limitations of solar PV lead to inevitably higher reserve capacity needs during winter months as reliance on RES increases. These types of insights are essential to develop targeted strategies

519 that enhance grid resilience and ensure a stable energy supply throughout
520 the year.

521 5. Conclusions

522 This study ~~has explored the characterisation of RES droughts in the~~
523 ~~real-life transition from a wind-dominated system to a more balanced system~~
524 ~~with integrated solar PV . This has been done through the comparison over~~
525 ~~a 45-year period of three different datasets : one based on a hand-crafted~~
526 aimed to answer two key questions: Do generic datasets have sufficient skill
527 to reliably quantify RES drought events? How does the integration of solar
528 PV into a predominantly wind-based system alter the characteristics of RES
529 droughts? To address these questions, three datasets were compared: one
530 developed using a regionally validated model and two ~~based on a generic~~
531 ~~model, derived from the European C3S-Energy . The generic model has~~
532 ~~two versions, one using large-scale aggregated information, and one which~~
533 ~~includes the locations of farms as well (also considered in the validated~~
534 ~~model) dataset. The C3S-Energy datasets differ in their assumptions, one~~
535 assumes a homogeneous distribution of wind and solar PV across the region,
536 while the other includes the actual locations of RES farms. In contrast, the
537 regionally validated model accounts for farm locations and uses tailored wind
538 and solar PV models selected to represent the actual generation.

539 Our results ~~show that generic datasets present limitations in the quantification~~
540 ~~of RES droughts. Although the three datasets used capture overall trends in~~
541 ~~drought occurrence demonstrate that datasets without regional validation~~
542 have notable limitations in quantifying RES drought events. While all three
543 datasets capture broad trends, significant differences ~~emerge when using~~
544 ~~non-tailored data for the study arise in extreme event assessment. In particular,~~
545 datasets without regional validation tend to underestimate the return periods
546 of RES droughts. This finding highlights that the choice of dataset and
547 its underlying assumptions, which ~~can lead to consequential differences in~~
548 ~~estimated RES drought characteristics, emphasising the need for datasets~~
549 ~~that are specifically designed for extreme event analysis.~~

550 This study reveals that differences in model parametrisation, particularly
551 ~~in the representation of wind turbine power curves~~ insufficient reserve capacity
552 planning and potential risks to grid stability and security of supply. This
553 highlights the critical need for regionally validated datasets when studying
554 RES droughts in renewable energy planning. The inclusion of wind and solar

555 PV panel characteristics, have a stronger influence on the drought estimates
556 than the inclusion of RES farm locations. The use of a validated dataset with
557 a carefully selected farm locations has a limited impact on RES drought
558 analysis compared to the choice of wind turbine power curve consistently
559 produced higher return periods and a greater number of drought events for
560 wind energy than the datasets derived from C3S-Energy. This suggests that
561 fine-tuning model parameters to match observed data is crucial for accurately
562 quantifying RES drought risks, thereby supporting more effective energy
563 system planning curves and solar PV models.

564 Finally, ~~the effect on RES droughts~~ The effect of the integration of so-
565 lar PV in a wind-dominated system on RES droughts has been explored ~~in~~
566 ~~a real-case setting. In the presented example of Ireland, the~~ Our anal-
567 ysis has demonstrated that transitioning to a ~~more balanced system with~~
568 ~~similar system with more equal~~ amounts of wind and solar PV ~~markedly~~
569 capacity reduces the frequency, duration, and seasonal variability of RES
570 drought events. This improvement is attributed to the complementary na-
571 ture of wind and solar PV generation, as solar PV generation typically peaks
572 in summer while wind generation is more consistent in winter. ~~Thus~~ However,
573 this integration is unable to counter the critical winter RES droughts, which
574 coincide with the strongest electricity demand in Northern European countries.
575 Still, a more diversified renewable energy mix ~~not only mitigates extreme~~
576 ~~drought conditions but also mitigates extreme~~ RES drought conditions and
577 enhances overall system resilience, providing valuable insights for policymakers
578 tasked with ensuring energy security.

579 The results presented in this study have ~~several limitations. Although~~
580 ~~ERA5 is among the best reanalysis datasets for renewable energy analysis;~~
581 ~~it still presents some biases, and its resolution may not capture local-scale~~
582 ~~phenomena. This is especially limiting if individual farms are considered, but~~
583 ~~its still shows good skill at statistically representing nation-wide behaviours~~
584 ~~considering the distribution of farms. Moreover, the methodology employs~~
585 four main limitations. First, the presented study uses a fixed threshold
586 to define RES drought events, ~~which is necessary for comparing the three~~
587 ~~datasets considering only weather-derived drivers, but does not account for~~
588 ~~demand variations. Consequently, while this approach enables a consistent~~
589 ~~inter-comparison, it will not signal events that are most critical for power~~
590 ~~system operations for their mismatch of RES generation and demand~~ but
591 other methods such as ones using the percentile of the generation could
592 yield different results. Second, the definition of RES droughts based on

generation does not consider the important role of demand, which could be of interest to system operators. Third, recent solar PV capacity expansions have changed the generation profile, limiting solar PV data for model training to a single year, whereas a longer validation period would be preferable. Lastly, the source for weather data is ERA5, which is among the best reanalysis datasets for renewable energy applications, but still comes in a limited spatial resolution, an issue that can be addressed once higher resolution datasets become available.

Future work is planned to extend the current analysis. First, climate projection data will be integrated with different energy scenarios, incorporating the addition of offshore wind, to better understand how climate change might affect RES droughts. Second, expanding the geographic domain of the study to include the rest of Europe would provide a more comprehensive understanding of RES droughts in an interconnected electricity grid. This would require extensive verification across other European countries, making it a more complex but highly relevant challenge.

Data Availability

The ERA5 data can be obtained from the Climate Data Store (<https://doi.org/10.24381/cds.adbb2d47>). The C3SE dataset is also available from the Climate Data Store (<https://doi.org/10.24381/cds.4bd77450>). Information on wind and solar PV farms in Ireland can be obtained from the EirGrid website (<https://www.eirgrid.ie/grid/system-and-renewable-data-reports>). The Atlite model used in this study is open-source and can be found on GitHub (<https://github.com/pypsa/atlite>). The data and code required to reproduce the analysis in this article will be made available upon acceptance of the manuscript in a public GitHub repository.

Acknowledgments

The research conducted in this publication was funded by Science Foundation Ireland and co-funding partners under grant number 21/SPP/3756 through the NexSys Strategic Partnership Programme.

References

- [1] EuroStat, Renewable Energy Statistics, 2023. URL: https://ec.europa.eu/eurostat/statistics-explained/index.php?title=Renewable_energy_statistics, Accessed: 2024-11-06.
- [2] H. C. Bloomfield, D. J. Brayshaw, L. C. Shaffrey, P. J. Coker, H. E. Thornton, Quantifying the increasing sensitivity of power systems to climate variability, *Environmental Research Letters* 11 (2016) 124025. doi:10.1088/1748-9326/11/12/124025.
- [3] H. C. Bloomfield, D. J. Brayshaw, A. Troccoli, C. M. Goodess, M. De Felice, L. Dubus, P. E. Bett, Y.-M. Saint-Drenan, Quantifying the sensitivity of european power systems to energy scenarios and climate change projections, *Renewable Energy* 164 (2021) 1062–1075. doi:10.1016/j.renene.2020.09.125.
- [4] F. Kaspar, M. Borsche, U. Pfeifroth, J. Trentmann, J. Drücke, P. Becker, A climatological assessment of balancing effects and shortfall risks of photovoltaics and wind energy in germany and europe, *Advances in Science and Research* 16 (2019) 119–128. doi:10.5194/asr-16-119-2019.
- [5] F. Mockert, C. M. Grams, T. Brown, F. Neumann, Meteorological conditions during periods of low wind speed and insolation in Germany: The role of weather regimes, *Meteorological Applications* 30 (2023) e2141. doi:10.1002/met.2141.
- [6] M. Ohba, Y. Kanno, D. Nohara, Climatology of dark doldrums in japan, *Renewable and Sustainable Energy Reviews* 155 (2022) 111927. doi:10.1016/j.rser.2021.111927.
- [7] M. J. Mayer, B. Biró, B. Szűcs, A. Aszódi, Probabilistic modeling of future electricity systems with high renewable energy penetration using machine learning, *Applied Energy* 336 (2023) 120801. doi:10.1016/j.apenergy.2023.120801.
- [8] D. Raynaud, B. Hingray, B. François, J. Creutin, Energy droughts from variable renewable energy sources in European climates, *Renewable Energy* 125 (2018) 578–589. doi:<https://doi.org/10.1016/j.renene.2018.02.130>.

- [9] A. Gangopadhyay, A. K. Seshadri, N. J. Sparks, R. Toumi, The role of wind-solar hybrid plants in mitigating renewable energy-droughts, *Renewable Energy* 194 (2022) 926–937. doi:10.1016/j.renene.2022.05.122.
- [10] J. Kapica, J. Jurasz, F. A. Canales, H. Bloomfield, M. Guezgouz, M. De Felice, Z. Kobus, The potential impact of climate change on european renewable energy droughts, *Renewable and Sustainable Energy Reviews* 189 (2024) 114011. doi:10.1016/j.rser.2023.114011.
- [11] K. Z. Rinaldi, J. A. Dowling, T. H. Ruggles, K. Caldeira, N. S. Lewis, Wind and Solar Resource Droughts in California Highlight the Benefits of Long-Term Storage and Integration with the Western Interconnect, *Environmental Science and Technology* 55 (2021) 6214–6226. doi:10.1021/acs.est.0c07848.
- [12] P. T. Brown, D. J. Farnham, K. Caldeira, Meteorology and climatology of historical weekly wind and solar power resource droughts over western North America in ERA5, *SN Applied Sciences* 3 (2021) 814. doi:10.1007/s42452-021-04794-z.
- [13] S. Allen, N. Otero, Standardised indices to monitor energy droughts, *Renewable Energy* 217 (2023) 119206. doi:10.1016/j.renene.2023.119206.
- [14] C. Bracken, N. Voisin, C. D. Burleyson, A. M. Campbell, Z. J. Hou, D. Broman, Standardized benchmark of historical compound wind and solar energy droughts across the Continental United States, *Renewable Energy* 220 (2024) 119550. doi:https://doi.org/10.1016/j.renene.2023.119550.
- [15] H. Lei, P. Liu, Q. Cheng, H. Xu, W. Liu, Y. Zheng, X. Chen, Y. Zhou, Frequency, duration, severity of energy drought and its propagation in hydro-wind-photovoltaic complementary systems, *Renewable Energy* (2024) 120845. doi:10.1016/j.renene.2024.120845, 2.
- [16] H. Hersbach, B. Bell, P. Berrisford, S. Hirahara, A. Horányi, J. Muñoz-Sabater, J. Nicolas, C. Peubey, R. Radu, D. Schepers, et al., The ERA5 global reanalysis, *Quarterly Journal of the Royal Meteorological Society* 146 (2020) 1999–2049. doi:10.1002/qj.3803.

- [17] L. Dubus, Y. Saint-Drenan, A. Troccoli, M. De Felice, Y. Moreau, L. Ho-Tran, C. Goodess, R. Amaro E Silva, L. Sanger, C3S Energy: A climate service for the provision of power supply and demand indicators for Europe based on the ERA5 reanalysis and ENTSO-E data, *Meteorological Applications* 30 (2023) e2145. doi:10.1002/met.2145.
- [18] F. Hofmann, J. Hampp, F. Neumann, T. Brown, J. Hörsch, Atlite: a lightweight Python package for calculating renewable power potentials and time series, *Journal of Open Source Software* 6 (2021) 3294. doi:10.21105/joss.03294.
- [19] A. Kies, B. U. Schyska, M. Bilousova, O. El Sayed, J. Jurasz, H. Stoecker, Critical review of renewable generation datasets and their implications for european power system models, *Renewable and Sustainable Energy Reviews* 152 (2021) 111614. doi:10.1016/j.rser.2021.111614.
- [20] EirGrid & SONI, System and Renewable Data Reports, 2023. URL: <https://www.eirgrid.ie/grid/system-and-renewable-data-reports>, Accessed: 2024-11-06.
- [21] Y.-M. Saint-Drenan, L. Wald, T. Ranchin, L. Dubus, A. Troccoli, An approach for the estimation of the aggregated photovoltaic power generated in several European countries from meteorological data, *Advances in Science and Research* 15 (2018) 51–62. doi:10.5194/asr-15-51-2018.
- [22] I. Staffell, S. Pfenninger, Using bias-corrected reanalysis to simulate current and future wind power output, *Energy* 114 (2016) 1224–1239. doi:10.1016/j.energy.2016.08.068.
- [23] Government of Ireland, Climate Action Plan 2024, Technical Report 3, Department of the Environment, Climate and Communications, 2023. URL: <https://www.gov.ie/pdf/?file=https://assets.gov.ie/284675/70922dc5-1480-4c2e-830e-295afd0b5356.pdf>, Accessed: 2024-11-06.
- [24] Sustainable Energy Authority Ireland, National Energy Projections 2024, Technical Report, Sustainability Energy Authority of Ireland,

721 2024. URL: <https://www.seai.ie/news-and-events/news/energy-projections-report>, Accessed: 2024-11-06.
722
723 [25] H. G. Beyer, G. Heilscher, S. Bofinger, A robust model for the mpp
724 performance of different types of pv-modules applied for the performance
725 check of grid connected systems, Eurosun (2004) 8.